A Comprehensive Approach for Multi-channel Image Registration

G. K. Rohde[1], S. Pajevic[2], C. Pierpaoli[1], and P. J. Basser[1]

[1] STBB/LIMB/NICHD
[2] MSCL/CIT
National Institutes of Health, Bethesda, MD, USA.

Abstract. We describe a general framework for multi-channel image registration. A new similarity measure for registering two multi-channel images, each with an arbitrary number of channels, is proposed. Results show that image registration performed based on different channels generates different results. In addition, we show that, when available, the inclusion of multi-channel data in the registration procedure helps produce more accurate results.

1 Introduction

The increasing popularity of new medical imaging modalities capable of producing multivariate data such as Diffusion Tensor MRI (DT-MRI), chemical shift imaging (CSI), phase contrast magnetic resonance angiography, etc., has brought about the need for image registration techniques capable of dealing with multi-channel images. Moreover, existing multi-modal registration techniques (see [1], [2], [3], [4]) can be used to generate multi-channel (multivariate) images from different types of scalar images of a single subject, i.e. conventional MRI and CT scans. All such multi-channel images can benefit from accurate multi-channel image registration procedures. The hope is that the additional information contained in multi-channel images can help render the registration process more accurate. Multiple image channels can be used to characterize each image location more uniquely. Thus unique correspondences between locations of two images are more likely, helping to avoid local optima during registration.

Most existing multi-channel image registration methods are specific to registration of DT-MRI images. Alexander *et al* [5],[6], investigated tensor similarity measures and reorientation approaches to be used when registering DT-MRI data. They reported that a tensor component difference measure combined with the preservation of principal direction tensor reorientation scheme (since tensors contain directional information they must be appropriately reoriented upon spatial transformation of the images) performed best among all options tried [5],[6]. Ruiz-Alzola *et al* [7] demonstrated the feasibility of an approach based on the correlation coefficient of tensor elements as an intensity based similarity function for registration of DT-MRIs. Recently, Guimond *et al* [8] investigated the use of a multivariate version of the daemons algorithm [9]for registering DT-MRI

data. Also worth noting is the work by Boes *et al* [10] where the authors used a multivariate mutual information similarity measure to register a scalar image to another set of two images of the same subject.

Here we describe a general framework for registering multi-channel images. A new measure of similarity for two multi-channel images each with an arbitrary number of channels is proposed. We investigate the use of the new method in registering DT-MRI data using both affine and higher order elastic transformations. Experiments using real and simulated datasets show that registration performed based on multiple image channels produces more accurate results than single channel registration.

2 Theory

The goal in image registration is to produce a mapping function $f: \mathbf{x} \rightarrow \mathbf{x}^{'}$ that transforms the spatial coordinates $\mathbf{x}$ of a target image $\mathbf{T}$ to the spatial coordinates $\mathbf{x}^{'}$ of a source image $\mathbf{S}$. For the source and target images to be registered the mapping function f should be chosen in such a way as to maximize some similarity measure (minimize some cost function) between the two images. Mathematically, the image registration problem can be stated as:

$$\max_{f} I(\mathbf{S}(f(\mathbf{x})), \mathbf{T}(\mathbf{x}), f) \tag{1}$$

where $I(\cdot, \cdot)$ represents the chosen similarity measure or cost function. Because of efficiency or accuracy considerations, the multi-channel images $\mathbf{T}$ and $\mathbf{S}$ may be first preprocessed in order to yield best results.

The multi-channel registration problem is described in Figure 1. Multi-channel images are first subjected to a preprocessing step. As described later, this step can either reduce or augment the number of image channels, depending upon the application. Next the images are registered using a multi-channel algorithm soon to be described. Once the spatial transformation that registers the images has been computed, it is applied to the original data and any necessary post processing operation is then performed for final output. The next few sections describe preprocessing approaches, a similarity measure, optimization and approaches for multichannel image registration.

2.1 Preprocessing

The objective of this step is is to transform the original data into images more suitable for registration. When the number of channels is too large, for example, it may be reduced by eliminating any redundant information in the original data using principal component analysis, independent component analysis, or some other kind of dimension reduction or feature extraction technique. Dimension augmentation may be used when the original image channels are not enough to characterize each image region uniquely. Wavelets, for example, could be used to create low-pass and high-pass image channels. Figure 1 depicts this step graphically.

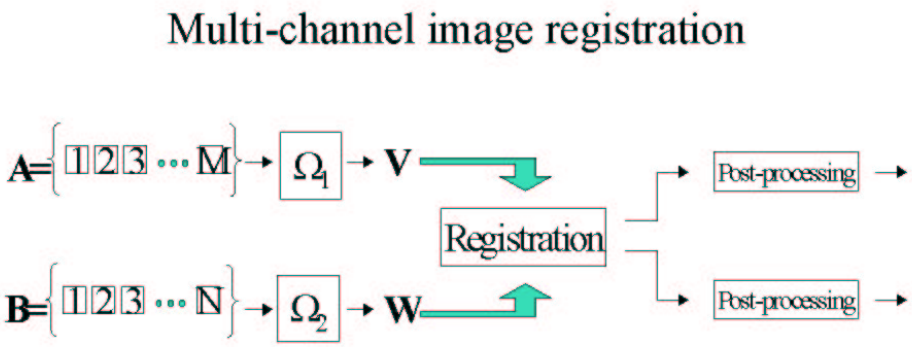

Fig. 1. Description of the possible steps in the multi-channel image registration process. Original images **A** and **B** with M and N channels each are passed through a dimension adjustment operations Ω_1 and Ω_2 producing images **V** and **W**, with P and Q channels, respectively. Images **V** and **W** are then used for registration.

2.2 Similarity measure

A common methodology used in voxel-based image registration has been to assume that the images are optimally aligned when the statistical dependency between their intensity values is highest. Strategies using least squares, correlation coefficient, and more recently mutual information ([1],[2],[3],[4]), have been used in single or multi-modality registration problems. Here we extend this methodology to the multi-channel registration problem.

Because of the high computational costs associated with estimating the multivariate mutual information between two images with an arbitrary number of channels each, we use the following measure of image similarity:

$$I(\mathbf{S},\mathbf{T}) = \frac{1}{2} log\left(\frac{|\Sigma_{\mathbf{S}}||\Sigma_{\mathbf{T}}|}{|\Sigma|}\right). \tag{2}$$

In equation (2), $|\Sigma|$ is the determinant of joint covariance matrix of multivariate random variables **T** and **S**, given by

$$|\Sigma| = \begin{vmatrix} \Sigma_{\mathbf{T}} & \Sigma_{\mathbf{ST}} \\ \Sigma_{\mathbf{ST}}^T & \Sigma_{\mathbf{S}} \end{vmatrix}. \tag{3}$$

Equation (2) is the multivariate mutual information for normally distributed multivariate random variables **T** and **S** [11]. Note that the computation expressed in equation (2) is much less demanding than estimating the general multivariate mutual information. In particular, when memory requirements are considered, the estimation of the joint probability density function via joint histogram computation for two multi-channel images is prohibitive. In contrast, the memory requirements for computing (2) are negligible, while the most expensive

computations involved are the inner products necessary to compute the elements of Σ.

The drawbacks associated with the use of similarity measure (2) stem from the fact that the intensity value of most images are not normally distributed. Therefore it is useful to investigate other interpretations of (2). Using $\Sigma = \mathbf{DPD}$ where $\mathbf{P}$ is a matrix of correlation coefficients and $\mathbf{D}$ is a diagonal matrix of standard deviations, one can show that under fairly weak assumptions (2) may be interpreted as a monotonic function of $|\mathbf{P}|$ such that $I(\mathbf{S}, \mathbf{T}) = -\frac{1}{2}\log(k|\mathbf{P}|)$, where k is the proportionality constant (see appendix A). Thus optimizing (2) can be thought of as maximizing the linear correlation coefficient between corresponding channels of each image while minimizing the correlation of channels that do not correspond. We point out that the use of equation (2) to measure image alignment is justified if it can be assumed that there is a linear relationship between the intensity values of the channels of each image being registered.

2.3 Optimization approaches

The first step in aligning two different images is usually an affine registration step. We use an algorithm similar to what is described in [3] to search for the 12 parameter affine transformation that maximizes Eq. (2). Subsequent elastic registration of the images is performed using the adaptive bases algorithm [12],[13]. The adaptive bases method uses sets of compactly supported radial basis functions to search for the elastic transformation $f(\mathbf{x})$ iteratively through different image resolutions. Note that the optimization of the spatial transformation $f(\mathbf{x})$ here is not crucial and other methods such as described by [14] could be used.

3 Validation Methods

Validation of image registration results, particularly nonrigid ones, is difficult because of the lack of a gold standard. Therefore we resort to indirect measures of alignment. In a first experiment we register a set of 7 images of different healthy volunteers to an 8th image chosen at random. The images used in this experiment are 3D DT-MRI images with three channels each (see description bellow). For comparison purposes, registration of each multi-channel image was performed using one individual image channel at a time as well as all the image channels combined using the multi-channel method previously described; remember, the approach described above allows for registration of images each with an arbitrary number of channels. Thus, by using four different registration methods, we generated 4 sets of 7 multi-channel images each. The first three sets contain multi-channel images that were registered to the template image using a single-channel approach based on channels 1,2, and 3, respectively. The fourth set of images contains the multi-channel images registered to the template using information from all 3 channels simultaneously. In order to determine which set of images was best aligned we use an approach similar to the one described in [15].

We calculate the variance for i^{th} voxel and j^{th} channel, $V(i,j,s)$ across all images in the same set, s. Then we use an average over all voxels to calculate the average variance for each channel $V_c(j,s) = (ni)^{-1} \sum_i V(i,j,s)$, where ni is the number of voxels, and the total average $V_a(s) = (nj)^{-1} \sum_j V_c(j,s)$, where nj is the number of channels. Note that in order to show relative improvement we report $V_c(j,s)$ as $\frac{V_c(j,s)}{V_c(j,0)}$, where $V_c(j,0)$ is the average variance of the unregistered set. The assumption is that V_c and V_a will be the smallest when the images are optimally aligned.

In a second experiment, a set of 10 3D target multi-channel images was created by applying 10 known transformations to a selected source multi-channel image. Normally distributed noise of variance 8 was added to each generated image whose intensity values ranged from 0 to 255. The transformations were generated using a set of randomly selected Wendland [16] radial basis functions, while the registration algorithm uses one of Wu's [17] radial basis functions. The nonrigid registration algorithm was then used to recover the known transformation using each individual image channel as well as all image channels combined for evaluation of the similarity measure. In addition to multi-channel similarity measure (2) we also used the standard correlation coefficient ρ between all the available image channels to register the images. Thus, in total, we compare 5 methods of registration. Note that due to the limited number of degrees of freedom used in the nonrigid registration algorithm, and the fact that the simulated deformation fields were generated using different basis functions than used in the adaptive bases algorithm, none of the methods can be expected to recover the known transformation without error. Thus we are able to compare the error between the simulated deformations and deformations generated by different registration methods. Note that a similar experimental procedure was used in [18]

4 DT-MRI

All imaging studies were performed with a 1.5 T GE Signa magnet, equipped with a whole-body gradient coil able to produce gradient pulses up to 50mT/m (GE Medical Systems, Milwaukee, WI). The acquisition parameters used are similar to those described in [19].All subjects used in the following experiments were healthy volunteers, both male and female, with ages between 22 and 53. After acquisition the diffusion weighted images were corrected for patient motion and eddy-current induced image distortion using the mutual information based registration approach described in [20].

The multi-channel images were composed of different rotationally invariant scalars extracted from the apparent diffusion tensor model described in [21],[22]. Channel 1 contains the trace of the tensor, channel 2 the relative anisotropy index, and channel 3 the skewness measure. One byte was used to represent the intensity values of each channel. These three specific channels were chosen because the correlation between them is low, implying that each channel contains unique information that is not present in other channels.

5 Results

Figure 2 contains the plot of the multivariate similarity measure (2) as a function of image rotation. The target and source images were generated from a single dataset by adding Gaussian noise as described earlier. The images were then rotated with respect to each other and the value of the multi-channel similarity measure (2) is plotted. Note the slight discontinuities around the local extrema are consistent with known effects of image interpolation in registration with mutual information-type cost functions [23].

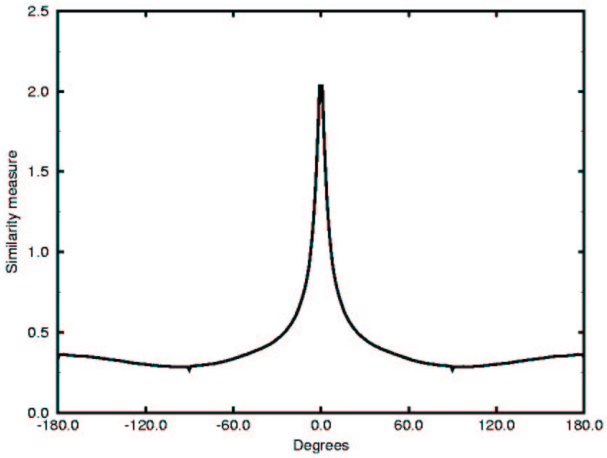

Fig. 2. Plot of multi-channel similarity measure as a function of image rotation.

Table 1 shows the relative improvement in average variance after correction with all approaches mentioned above. Note that only affine transformations were used to align the images in this experiment. When considering the variance of all channels, the multi-channel approach produces best results. The superiority of the multi-channel approach is even more evident when higher order elastic transformations are used (see table2). Figure 3 displays the average of the 7 multi-channel images before and after registration with our approach. The average image of each channel is significantly sharper after registration, indicating good overall alignment of the images.

Table 3 displays the average pixel error for the simulated registration experiments. Evidently, the registration procedure that uses Eq. (2) as similarity measure outperforms all others, including the standard correlation coefficient ρ between all image channels. This suggests that the relationship between unlike, as well as like, channels is important during multi-channel image registration.

Table 1. Relative variance for each image channel after affine registration with single and multi-channel approaches.

	$V_c(1,s)$	$V_c(2,s)$	$V_c(3,s)$	$V_a(s)$
ch. 1 registration	0.388	0.430	0.481	0.433
ch. 2 registration	0.507	0.375	0.406	0.430
ch. 3 registration	0.588	0.387	0.404	0.460
multi-channel reg.	0.414	0.397	0.440	0.417

Table 2. Relative variance for each image channel after elastic registration with single and multi-channel approaches.

	$V_c(1,s)$	$V_c(2,s)$	$V_c(3,s)$	$V_a(s)$
ch. 1 registration	0.287	0.404	0.474	0.387
ch. 2 registration	0.441	0.354	0.392	0.397
ch. 3 registration	0.630	0.401	0.396	0.473
multi-channel reg.	0.300	0.350	0.395	0.350

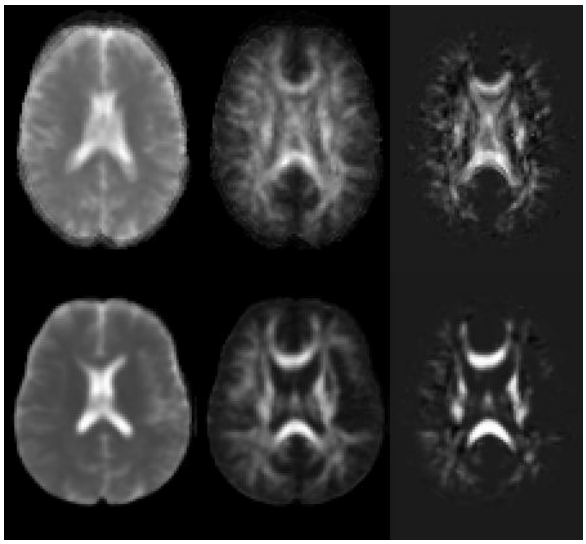

Fig. 3. Average of 7 multi-channel images before and after elastic registration using our multi-channel approach. Each row, from left to right: Trace channel, anisotropy channel, skewness channel.

Table 3. Average pixel error after registration using several methods.

	ch. 1	ch. 2	ch. 3	ρ	Eq. [2]
trial 1	1.55561	1.57457	2.05176	1.57586	1.39538
trial 2	1.86019	1.61742	2.16298	1.84785	1.53049
trial 3	1.64350	1.45177	1.87407	1.68824	1.37878
trial 4	1.60639	1.35870	1.69225	1.49407	1.34622
trial 5	1.63641	1.54283	2.21301	1.74026	1.35014
trial 6	1.54050	1.45536	1.82586	1.54400	1.35805
trial 7	1.68628	1.53352	1.61236	1.59638	1.41817
trial 8	1.66844	1.60115	2.19608	1.74772	1.37936
trial 9	1.76214	1.55805	2.09162	1.74509	1.51251
trial 10	1.76584	1.56465	2.09041	1.74318	1.41244

6 Conclusions

Here we have described a general framework for registering a multi-channel image with an arbitrary number of channels to another image also with an arbitrary number of channels using a multivariate correlation approach. Our approach not only considers the similarity between like-channels of each image, but also the similarity between channels that do not correspond. Although we have used diffusion tensor images of the human brain for validation, we believe our method to be applicable to many other multi-channel registration problems.

Results show that image alignment based on different image channels can lead to different registrations. This is true especially in the nonrigid case, but also for the affine one. When considering image alignment across all channels, results indicate that, even for the affine case, the use of all channels simultaneously using the similarity measure defined in Eq. [2] during registration is superior to any of the other methods investigated.

APPENDIX

We show that under fairly weak assumptions Eq. (2) is a monotonic function with respect to $|\mathbf{P}|$. Using $\Sigma = \mathbf{DPD}$, where $\mathbf{P}$ is a matrix of correlation coefficients and $\mathbf{D}$ is a diagonal matrix of standard deviations,

$$\mathbf{D} = \begin{pmatrix} \mathbf{D_T} & \mathbf{0} \\ \mathbf{0} & \mathbf{D_S} \end{pmatrix}, \tag{4}$$

Eq. (2) becomes

$$I(\mathbf{S}, \mathbf{T}) = \frac{1}{2} log \left(\frac{|\Sigma_\mathbf{S}||\Sigma_\mathbf{T}|}{|\mathbf{D}_\mathbf{S}^2||\mathbf{D}_\mathbf{T}^2||\mathbf{P}|} \right). \tag{5}$$

Note that $\frac{|\Sigma_\mathbf{T}|}{|\mathbf{D}_\mathbf{T}^2|}$ is constant in (5) because the target image is static throughout the registration procedure. If we assume that spatial transformations f do not change the covariance between the image channels of $\mathbf{S}$ significantly $\frac{|\Sigma_\mathbf{s}|}{|\mathbf{D}_\mathbf{s}^2|}$ is also

constant and (5) is a monotonic function with respect to $|\mathbf{P}|$. This assumption is reasonable for f modifies all image channels identically. Therefore one can expect the relationship between the image channels not to change significantly. Note also that if the image channels of $\mathbf{S}$ (and of $\mathbf{T}$) are uncorrelated further simplification is possible and (5) becomes $I(\mathbf{S}, \mathbf{T}) = -0.5 * log(|\mathbf{P}|)$.

Lastly, note that the multi-channel similarity measure (2) reduces to a monotonic function of the scalar correlation coefficient when the images have one channel each. In this case

$$|\Sigma| = \begin{pmatrix} Cov(\mathbf{S}, \mathbf{S}) & Cov(\mathbf{S}, \mathbf{T}) \\ Cov(\mathbf{T}, \mathbf{S}) & Cov(\mathbf{T}, \mathbf{T}) \end{pmatrix} \tag{6}$$

and (2) reduces to $I(\mathbf{S}, \mathbf{T}) = -0.5 * log(1-\rho)$, where ρ is the correlation coefficient between the intensity values of the images.

References

1. Viola, P., Wells, III, W. M.: Alignment by maximization of mutual information. Proc. Int. Conf. Computer Vision, Boston (1995) 16–23
2. Wells, III, W. M., Viola, P., Atsumi, H., Nakajima, S., Kininis, R.: Multi-modal volume registration by maximization of mutual information. Medical Image Analysis. **1** (1996) 35–51
3. Maes, F., Collignon, A., Vandermeulen, D., Marcha, G., Suetens, P.: Multimodality image registration by maximization of mutual information. IEEE Transactions on Medical Imaging **16** (1997) 187–198
4. Studholme, C., Hill, D. L. J., Hawkes, D. J.: Automated trhee-dimensional registration of magnetic resonance and positron emission tomography brain images by multiresolution optimization of voxel similarity measures. Medical Physics **24** (1997) 25–35
5. Alexander, D. C., Gee, J. C., Bajcsy, R: Transformations of and similarity measures for diffusion tensor MRIs. Workshop on Biomedical Image Registration, at CAIP (1999)
6. Alexander, D. C., Pierpaoli, C., Basser, P. J, Gee, J. C: Spatial Transformations of Diffusion Tensor Magnetic Resonance Images. IEEE Transactions on Medical Imaging **20** (2001) 1131–1139
7. Ruiz-Alzola, J., Westin, C.-F, Warfield, S. K., Alberola, C., Maier, S., Kinikis, R: Nonrigid registration of 3D tensor medical data. Medical Image Analysis **6** (2002) 143–161
8. Guimond, A., Guttmann, C. R. G., Warfield, S. K., Westin, C.-F: Deformable registration of DT-MRI data based on transformation invariant tensor characteristics. Proc. ISBI'02 (2002)
9. Thirion, J.-P: Image matching as a diffusion process: an analogy with Maxwell's daemons. Medical Image Analysis, **2** (1998) 243–260
10. Boes, J. L., Meyer, C. R.: Multi-variate mutual information for registration. Proc. MICCAI'99 (1999) 606–612
11. Salomon Kullback: Information Theory and Statistics. Dover Publications, Mineola, New York (1968)
12. Rohde, G. K., Aldroubi, A., Dawant, B. M.: The adaptive bases algorithm for nonrigid image registration. Proc. SPIE Medical Imaging, San Diego, USA (2002)

13. Rohde, G. K.: The adaptive grid registration algorithm: a new spline modeling approach for automatic intensity based nonrigid registration. Masters thesis, Dept. Electrical Engineering, Vanderbilt University (2001)
14. Rueckert, D., Sonoda, L. I., Hayes, C., Hill, D. L. G., Leach, M. O., Hawkes, D. J.: Nonrigid registration using free-form deformations: application to breast MR images. IEEE Transactions on Medical Imaging **18** (1999) 712–721
15. Studholme, C., Cardenas, V. A., Weiner, M. W.: Multiscale image and multiscale deformation of brain anatomy for building average brain atlases. Proc. SPIE Medical Imaging, Sand Diego, USA (2001)
16. Wendland, H.: Piecewise polynomial, positive definite and compactly supported radial basis functions of minimal degree. Advances in Computational Mathematics, **4** (1995) 389–396
17. Schaback, R., Creating surfaces from scattered data using radial basis functions. in Mathematical Models for Curves and Surfaces. Vanderbilt University Press, Nashville, TN (1995)
18. Rueckert, D., Clarkson, M. J., Hill, D., L., G., Hawkes, D., J.: Non-rigid registration using higher-order mutual information. Proce SPIE Medical Imaging, San Diego, 2000.
19. Pierpaoli, C., Jezzard, P., Basser, P. J, Barbett, A., DiChiro, G.: Diffusion tensor imaging of the human brain. Radiology **201** (1996) 637–648
20. Rohde, G. K., Barnett, A., S., Basser, P., J., Marenco, S., Pierpaoli, C.: A comprehensive approach for correcting motion and distortion in diffusion weighted MRI. Proc 21st Southern Biomedical Engineering Conference, Bethesda, MD, (2002)
21. Basser, P. J., Mattiello, J., Lebihan, D.: MR Diffusion Tensor and Imaging. Biophysical Journal **66** (1994) 259–267
22. Basser, P. J.: New histological and physiological stains derived from diffusion-tensor MR images. Annals of the New York Academy of Sciences **820** (1997) 123–138
23. Pluim, J., Maintz, J.,Viergever, M.: Interpolation artifacts in mutual information-based image registration. Computer Vision and Image Understanding **77** (2000) 211–232